iMEDiTEC 2017

ORIGINAL PAPER

Fabrication of Nanoporosities on Metallic Glass Surface by Hydroxyapatite Mixed Edm for Orthopedic Application

A.A. Aliyu a, A.M. Abdul-Rani [a], *, T.L. Ginta [a], C. Prakash [b], E. Axinte c, aR. Fua-Nizan

[a] *Department of Mechanical Engineering, Universiti Teknologi PETRONAS, 31750 Bandar Seri Iskandar, Perak, Malaysia*
[b] *Department of Mechanical Engineering, UIET, Panjab University, Chandigarh, India*
c Gheorghe Asachi Technical University of Iasi (TUIASI) - Faculty of Machine Manufacturing and Industrial Management (CMMI), Department of Machine Manufacturing Technology

* *Corresponding author: majdi@utp.edu.my*

ABSTRACT

Bulk metallic glasses (BMGs) have exceptional biomechanical characteristics like low elastic modulus, outstanding fracture strength, superior wear and corrosion resistance compared to routinely used biomaterials. The major downside of BMG is its inability to osseointegrate to the surrounding living tissues. To solve this problem, a biocompatible and bone-like nanoporous layer are normally imparted on the implant surface. In this study, a very hard, biocompatible and nano-porous layer was deposited on the Zr-based metallic glass surface, by hydroxyapatite mixed electrical discharge machining (HA-EDM). FESEM was employed to observe the pore distribution, geometry, and sizes. The result reveals the formation of rough, narrow craters and interconnected nanoporosities in the range of 558.2 nm to 893 nm in diameter and surface area of 244764 nm2 to 626596 nm2. The surface produced by HA-EDM are expected to facilitate higher tissue ingrowth and bone-implant adhesion, compared to that of EDM.

INTRODUCTION

The long-term stability of orthopedic implant depends on several factors such as the implants material, manufacturing, design and the surface modification techniques. Biomaterials such as titanium and its alloys, cobalt chromium and stainless steel are the most frequently used orthopedic implant materials (Odekerken, Welting, Arts, Walenkamp, & Emans, 2013). Despite the higher strength of the metal based implant compared to the natural bone, most of the implants failed at the early stage of implantation (less than 15years). This period is comparatively shorter than the life span of human (even the elderly person with a life expectancy of 17.9 years) (Chen & Thouas, 2015). Thus, the patient most undergoes a revision surgery, which is not normally recommended due to the complexity of the process (Ashkanfar, Langton, & Joyce, 2017; DeFrances, Lucas, Buie, & Golosinskiy, 2008). The potential causes of this implant pre-mature failure may be due to several reasons such as incompatible mechanical properties of the implant or fixation device, the development of undesired osteointegration between living bone and the synthetic surface, poor implant surface finishing as well as poor corrosion and wear resistance (Ashkanfar et al., 2017; Bahraminasab et al., 2012; Martin & Trousdale, 2013). Fig. 1 shows the hip anatomy, components of the total hip replacement and the merged hip implant fits into the body. The number of hip or knee revision surgery is rising every year as depicted in Fig. 2. Kurtz, Ong, Lau, Mowat, and Halpern (2007) projected that the cases of total hip and knee revision surgery will rise with over 137% by 2030 in United State. Fig. 3 depicts a normal revised hip and the loose screw after revision surgery.

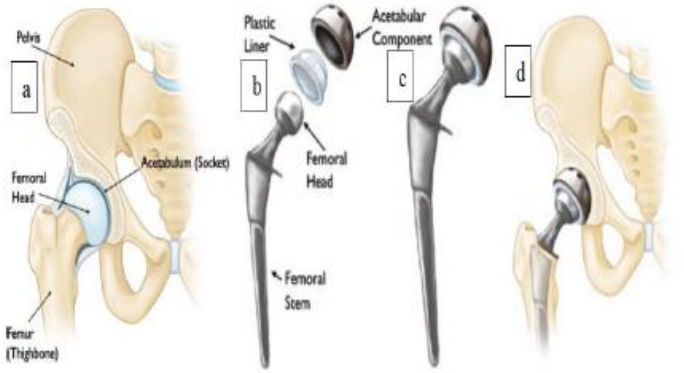

Fig. 1(a) Anatomy of normal hip (b) components of total hip replacement (c) Merged component (implant) (d) Implant fits into the body

OPEN ACCESS Freely available online
eISBN 978-967-0194-93-6 FBME

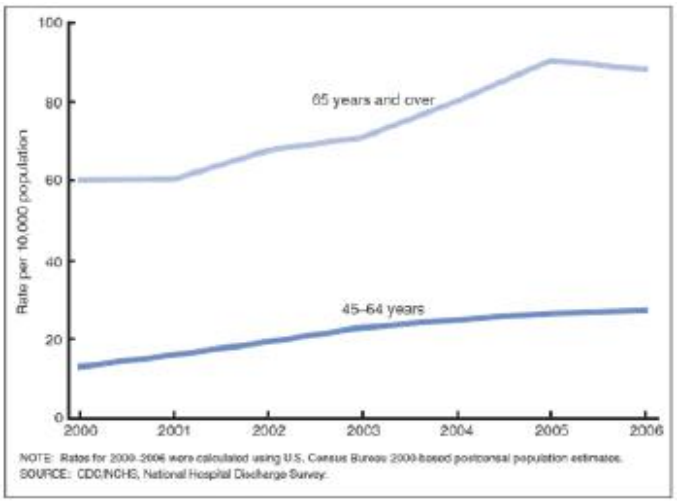

Fig. 2 rate of knee replacements in United States for hospital inpatients of 45 and above years old (2000 - 2006) (DeFrances et al., 2008).

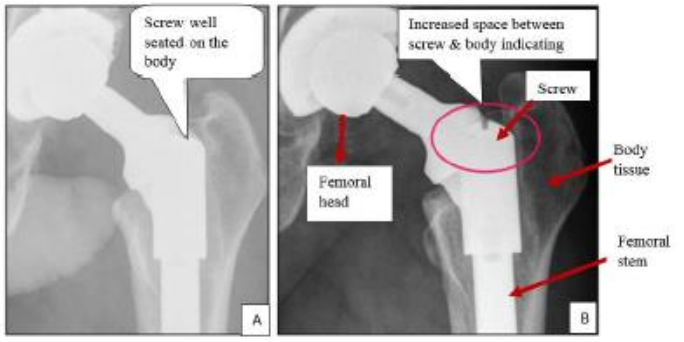

Fig. 3 Screw seated in the proximal body after revision surgery (A) A clear space between the screw and the proximal body, indicating loosening, 11 months after the index revision surgery (B) (Martin & Trousdale, 2013)

Bulk metallic glass (BMG) are non-crystalline alloys also called amorphous alloys (liquid metal), which have exceptional properties when compared with crystalline solids. BMGs are superior than the routinely used biomaterials (titanium alloys, cobalt-chromium, and stainless steel) in terms of strength, modulus of elasticity, wear and corrosion resistance as well as fatigue endurance (W.-H. Wang, Dong, & Shek, 2004). Thus, BMGs are continuously gaining attention by several researchers, especially in the biomedical area.

Despite the continuous emergence of new biomedical materials, there are still unsolved issues. For instance, BMG has a bio-inert oxide layer, which is characterized by low surface hardness and poor wear resistance. Thus, this layer does not promote strong physical bonding with the living tissues. Several authors considered coating the implant surface with a biocompatible, bioactive, and nanoporous layers through several kinds of coating methods as a primary solution to this problem (Odekerken et al., 2013; Stojanovic et al., 2007). Calcium phosphate (CaP) containing compounds, such as hydroxyapatite (HA) which contain the main inorganic component of the bone were adopted as coating material by many researchers (Asri, Harun, Hassan, Ghani, & Buyong, 2016; L.-N. Wang & Luo, 2011; Xu et al., 2016; Y. Zhang et al., 2014). CaP/HA surface coating increases the biocompatibility and provides a very tight bonding between the implant and the surrounding tissues (Asri et al., 2016; Dorozhkin, 2015). In addition, the porous layer is believed to have a reasonable and adjustable modulus of elasticity (Prakash, Kansal, Pabla, & Puri, 2015; L. Zhang, He, Zhang, Jiang, & Zhou, 2016). Among the hydroxyapatite deposition techniques, plasma spray is the most common and commercially available. However, this method is expensive, produces surface cracks and require very high temperature, which might change the initial performance of the substrate material. Powder mixed electric discharge machining (PMEDM) is an emerging technology which simultaneously acts as a machining and surface modification technique. The use of EDM in mold, tools, automobiles and aerospace industries have been largely documented (Amorim & Weingaertner, 2004; Cabanes, Portillo, Marcos, & Sánchez, 2008). Lately, the concept of material transfer from the tool and the dielectric additives to the workpiece surface during powder mixed EDM (PMEDM) process was reported by several authors (A. A. Aliyu, Hamidon, & Rohani, 2014; A. A. A. Aliyu, Rohani, Rani, & Musa, 2017; Batish, Bhattacharya, Singla, & Singh, 2012; Liew, Yan, & Kuriyagawa, 2013; Saxena, Agarwal, & Khare, 2016). Fig. 4 demonstrate the mechanism of material migration at machining zone during PMEDM of Zr-based BMG. In the present study Zr-based, BMG were machined using hydroxyapatite mixed electrical discharge machining (HA-EDM). FESEM was used to examine the HA-EDMed BMG surface. An extremely hard surface, with dense interconnected nano pores were fabricated.

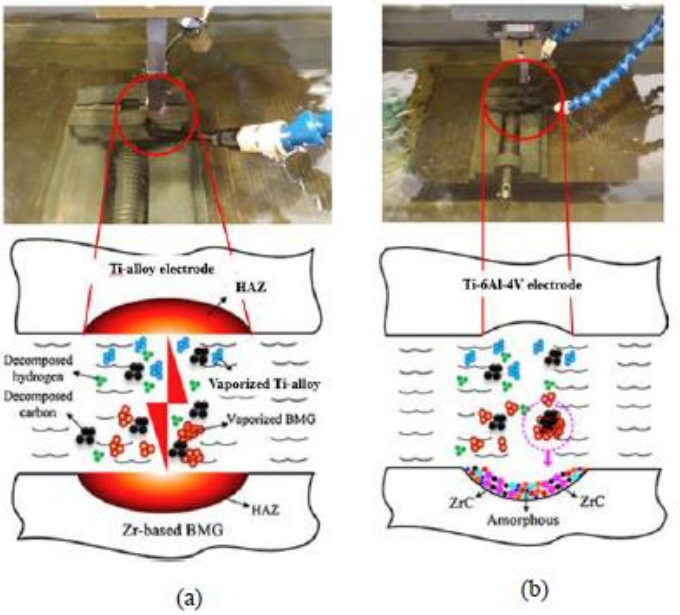

Fig. 4 PMEDM gap (a) discharge time: melting and vaporization of workpiece and tool materials (b) off-time: deposition of the carbide layer on the workpiece surface.

MATERIALS AND METHOD

5g/L of hydroxyapatite powder concentration was mixed with the hydrocarbon EDM oil in the fabricated 38.5L capacity PMEDM main tank. HA mixed EDM oil was circulated and conveyed to fabricated metallic machining tank (Fig. 5). A cuboidal shape 9 x 11 mm BMG was machined using the die sinker EDM machine and the 10 x 11 pure titanium electrode. A 2 level experimental design and 3 factors (discharge current (Dc), discharge time (Dt), and powder concentration (Ep)) gives a total of 8 experimental runs was carried out. Machining parameters and levels were summarized in Table 1. The HA-EDMed BMG surface was examined using Field Emission Scanning Electron Microscopy (FESEM). Fig. 6 shows the FESEM micrograph and EDX of the BMG (as received).

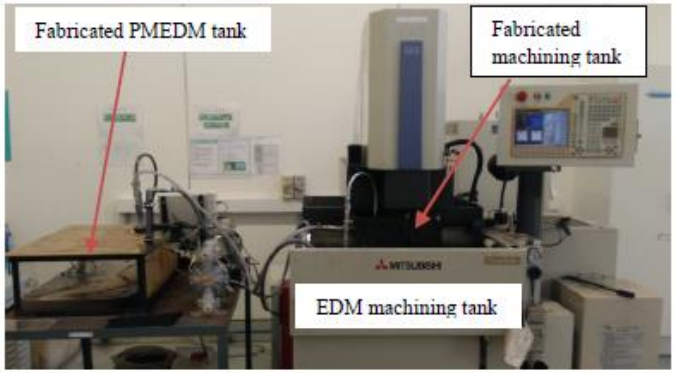

eISBN 978-967-0194-93-6 FBME

Fig. 5 Fabricated PMEDM sysem

Table 1 Machining conditions and respective levels

Machining conditions	Levels	
	1	2
Discharge current (A)	8	12
Discharge time (µs)	4	16
Powder concentration (g/L)	0	5

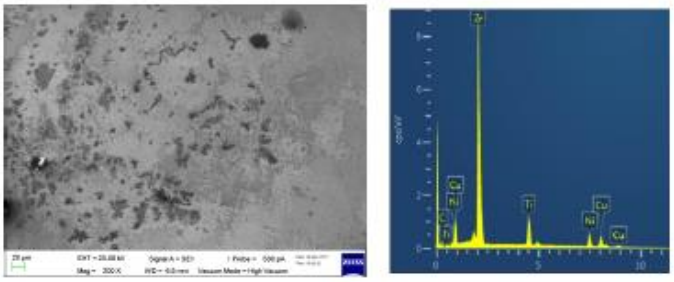

Fig. 6 FESEM micrograph of as received BMG

RESULTS AND DISCUSSION

FESEM micrographs of EDMed BMG and HA-EDMed BMG are depicted in Fig. 7. Numerous interconnected micro, submicro, and nano pores can be observed in both EDMed and HA-EDMed BMGs. However, the pores in the EDMed BMG (Fig. 7a) are scanty compared with HA-EDMed (Fig. 7b). This may be due hydroxyapatite powder added to the dielectric fluid and the low energy (Dc and Dt) used. The added powder stabilizes the EDM process by increasing the discharge gap and insulating the dielectric strength. In addition to porosities, a deep and wide craters could be noticed on the EDMed surface, while the craters are narrow, interconnected and shallow in the HA-EDMed surface. A pore size of 558.2 nm to 893 nm in diameter could be observed in the highly magnified micrograph of both EDMed and HA-EDMed BMG surface (Fig. 7c and 7d). This indicates that the addition of HA powder does not have much influence on the pore size. However, the pore surface area ranged between 244764 nm2 to 626596 nm2 were observed. The formation of different layers can be seen in Fig. 7e. The topmost layer is the extremely hard carbide layer, which is formed due to the reaction of carbon in the dielectric hydrocarbon fluid and the workpiece alloying elements. The recast and oxide film constituted the middle layers. The recast layer is produced because of re-solidification of unflushed metallic debris in the craters (Kruth, Stevens, Froyen, & Lauwers, 1995). The last layer is the heat affected zone, (heated but non-melted layer). This layer is formed due to heating and subsequent quenching during the EDM process.

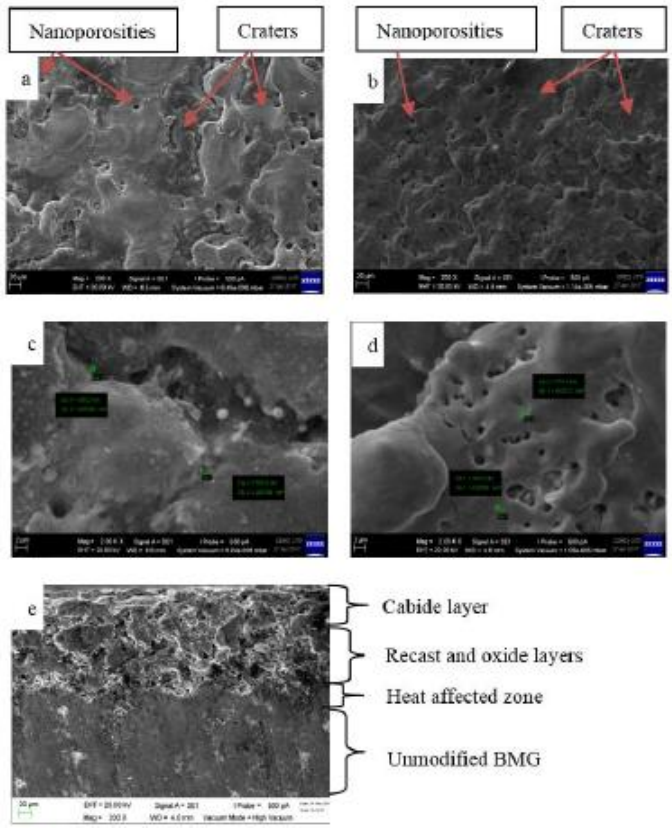

Fig. 7 FESEM micrograph of (a) EDMed BMG (Dc = 12A, Dt = 16µs, Pc = 0) (b) HA-EDMed BMG (Dc = 8.0A, Dt = 4.0µs, Pc = 5) (c) pore size of EDMed BMG (d) pore size of HA-EDMed BMG (e) sectional view of HA-EDMed BMG.

CONCLUSION

It can be concluded that EDM machine is suitable for not only fabricating implant but also imparting a nanoporous on the implant surface. However, the addition of hydroxyapatite powder facilitates the formation of the nanopores and shallow craters. A low discharge current of 8.0A and discharge time of 4.0µs were found to have a great contribution to the formation of interconnected nanoporosities. Nanopores of about 558.2 nm to 893 nm diameter and 244764 nm2 to 626596 nm2 surface area were fabricated on the Zr-based BMG surface. The craters produced were larger and wider on the EDMed BMG surface compared to HA-EDMed surface. It is believed that nonoporosities and narrow craters implant surface fabricated by HA-EDM possess greater bone-implant adhesion, higher strength bonding and full tissue interlocking when compared with conventionally fabricated EDM surface with full in on the implant surface.

ACKNOWLEDGEMENT

The authors of this paper acknowledged the support of University Technology PETRONAS for providing all necessary facilities as well as financial support to carry out this research.

REFERENCES

Aliyu, A. A., Hamidon, M., & Rohani, J. M. (2014). Parametric Study of Powder Mixed Electrical Discharge Machining and Mathematical Modeling of SiSiC Using Copper Electrode. Paper presented at the Advanced Materials Research.

Aliyu, A. A. A., Rohani, J. M., Rani, A. M. A., & Musa, H. (2017). Optimization of electrical discharge machining parameters of sisic through response surface methodology. jurnal teknologi, 79(1), 119-129.

Amorim, F., & Weingaertner, W. (2004). Die-sinking electrical discharge machining of a high-strength copper-based alloy for injection

eISBN 978-967-0194-93-6 FBME

molds. Journal of the Brazilian Society of Mechanical Sciences and Engineering, 26(2), 137-144.
Ashkanfar, A., Langton, D. J., & Joyce, T. J. (2017). A large taper mismatch is one of the key factors behind high wear rates and failure at the taper junction of total hip replacements: A finite element wear analysis. Journal of the mechanical behavior of biomedical materials.
Asri, R., Harun, W., Hassan, M., Ghani, S., & Buyong, Z. (2016). A review of hydroxyapatite-based coating techniques: Sol–gel and electrochemical depositions on biocompatible metals. Journal of the mechanical behavior of biomedical materials, 57, 95-108.
Bahraminasab, M., Sahari, B., Edwards, K., Farahmand, F., Arumugam, M., & Hong, T. S. (2012). Aseptic loosening of femoral components–a review of current and future trends in materials used. Materials & Design, 42, 459-470.
Batish, A., Bhattacharya, A., Singla, V., & Singh, G. (2012). Study of material transfer mechanism in die steels using powder mixed electric discharge machining. Materials and Manufacturing Processes, 27(4), 449-456.
Cabanes, I., Portillo, E., Marcos, M., & Sánchez, J. (2008). An industrial application for on-line detection of instability and wire breakage in wire EDM. Journal of Materials Processing Technology, 195(1), 101-109.
Chen, Q., & Thouas, G. A. (2015). Metallic implant biomaterials. Materials Science and Engineering: R: Reports, 87, 1-57.
DeFrances, C. J., Lucas, C. A., Buie, V. C., & Golosinskiy, A. (2008). 2006 National hospital discharge survey. Natl Health Stat Report, 5, 1-20.
Dorozhkin, S. V. (2015). Calcium orthophosphate deposits: preparation, properties and biomedical applications. Materials Science and Engineering: C, 55, 272-326.
Kruth, J.-P., Stevens, L., Froyen, L., & Lauwers, B. (1995). Study of the white layer of a surface machined by die-sinking electro-discharge machining. CIRP Annals-Manufacturing Technology, 44(1), 169-172.
Kurtz, S., Ong, K., Lau, E., Mowat, F., & Halpern, M. (2007). Projections of primary and revision hip and knee arthroplasty in the United States from 2005 to 2030. J Bone Joint Surg Am, 89(4), 780-785.
Liew, P. J., Yan, J., & Kuriyagawa, T. (2013). Experimental investigation on material migration phenomena in micro-EDM of reaction-bonded silicon carbide. Applied Surface Science, 276, 731-743. doi:http://doi.org/10.1016/j.apsusc.2013.03.161
Martin, J. R., & Trousdale, R. T. (2013). Unique failure mechanism of a femoral component after revision total hip arthroplasty. Orthopedics, 36(10), e1327-e1329.
Odekerken, J. C., Welting, T. J., Arts, J. J., Walenkamp, G., & Emans, P. J. (2013). Modern orthopaedic implant coatings—their pro's, con's and evaluation methods. Modern surface engineering treatments. New York: InTech, 45-73.
Prakash, C., Kansal, H., Pabla, B., & Puri, S. (2015). Processing and Characterization of Novel Biomimetic Nanoporous Bioceramic Surface on β-Ti Implant by Powder Mixed Electric Discharge Machining. Journal of Materials Engineering and Performance, 24(9), 3622-3633.
Saxena, K. K., Agarwal, S., & Khare, S. K. (2016). Surface Characterization, Material Removal Mechanism and Material Migration Study of Micro EDM Process on Conductive SiC. Procedia CIRP, 42, 179-184. doi:http://dx.doi.org/10.1016/j.procir.2016.02.267
Stojanovic, D., Jokic, B., Veljovic, D., Petrovic, R., Uskokovic, P., & Janackovic, D. (2007). Bioactive glass–apatite composite coating for titanium implant synthesized by electrophoretic deposition. Journal of the European Ceramic Society, 27(2), 1595-1599.
Wang, L.-N., & Luo, J.-L. (2011). Preparation of hydroxyapatite coating on CoCrMo implant using an effective electrochemically-assisted deposition pretreatment. Materials Characterization, 62(11), 1076-1086.
Wang, W.-H., Dong, C., & Shek, C. (2004). Bulk metallic glasses. Materials Science and Engineering: R: Reports, 44(2), 45-89.
Xu, H., Geng, X., Liu, G., Xiao, J., Li, D., Zhang, Y., . . . Zhang, C. (2016). Deposition, nanostructure and phase composition of suspension plasma-sprayed hydroxyapatite coatings. Ceramics International, 42(7), 8684-8690.
Zhang, L., He, Z., Zhang, Y., Jiang, Y., & Zhou, R. (2016). Enhanced in vitro bioactivity of porous NiTi–HA composites with interconnected pore characteristics prepared by spark plasma sintering. Materials & Design, 101, 170-180.
Zhang, Y., Liu, Y., Shen, Y., Ji, R., Li, Z., & Zheng, C. (2014). Investigation on the influence of the dielectrics on the material removal characteristics of EDM. Journal of Materials Processing Technology, 214(5), 1052-1061.

OPEN ACCESS Freely available online
eISBN 978-967-0194-93-6 FBME